

# Extracting short distance information from $b \rightarrow s \ell^+ \ell^-$ effectively

Keith S. M. Lee,<sup>1</sup> Zoltan Ligeti,<sup>2</sup> Iain W. Stewart,<sup>3</sup> and Frank J. Tackmann<sup>2</sup>

<sup>1</sup>*California Institute of Technology, Pasadena, CA 91125*

<sup>2</sup>*Ernest Orlando Lawrence Berkeley National Laboratory, University of California, Berkeley, CA 94720*

<sup>3</sup>*Center for Theoretical Physics, Massachusetts Institute of Technology, Cambridge, MA 02139*

We point out that in inclusive  $B \rightarrow X_s \ell^+ \ell^-$  decay an angular decomposition provides a third ( $q^2$  dependent) observable sensitive to a different combination of Wilson coefficients than the rate and the forward-backward asymmetry. Since a precise measurement of  $q^2$  dependence requires large data sets, it is important to consider the data integrated over regions of  $q^2$ . We develop a strategy to extract all measurable Wilson coefficients in  $B \rightarrow X_s \ell^+ \ell^-$  from a few simple integrated rates in the low  $q^2$  region. A similar decomposition in  $B \rightarrow K^* \ell^+ \ell^-$ , together with the  $B \rightarrow K^* \gamma$  rate, also provides a determination of the Wilson coefficients, without reliance on form factor models and without having to measure the zero of the forward-backward asymmetry.

## I. INTRODUCTION

At the scale of  $B$  meson decays, flavor changing interactions at the electroweak scale and above are encoded in Wilson coefficients of operators of dimension five and higher. The main goal of the  $B$  physics program is to make overconstraining measurements of the magnitudes and phases of these coefficients [1], and thereby search for deviations from the standard model (SM).

The  $b \rightarrow s \ell^+ \ell^-$  process has been observed both in inclusive  $B \rightarrow X_s \ell^+ \ell^-$  [2, 3] and exclusive  $B \rightarrow K^{(*)} \ell^+ \ell^-$  [4, 5] decays. Throughout this paper we assume the SM except where explicitly stated otherwise. We also neglect the strange quark and lepton masses. Two observables that have been extensively discussed for inclusive  $B \rightarrow X_s \ell^+ \ell^-$  decay are the  $q^2$  spectrum [6] and the forward-backward asymmetry [7] (or, equivalently, the energy asymmetry [8]). At lowest order, they are

$$\frac{d\Gamma}{dq^2} = \Gamma_0 m_b^3 (1-s)^2 \left[ (|C_9|^2 + C_{10}^2)(1+2s) + \frac{4}{s} |C_7|^2 (2+s) + 12 \operatorname{Re}(C_7^* C_9) \right], \quad (1)$$

$$\begin{aligned} \frac{dA_{\text{FB}}}{dq^2} &= \int_{-1}^1 dz \frac{d^2\Gamma}{dq^2 dz} \operatorname{sgn}(z) \\ &= -3\Gamma_0 m_b^3 (1-s)^2 s C_{10} \operatorname{Re}\left(C_9 + \frac{2}{s} C_7\right). \end{aligned} \quad (2)$$

Here  $q^2 = (p_{\ell^+} + p_{\ell^-})^2$  is the dilepton invariant mass,  $s = q^2/m_b^2$ ,  $z = \cos\theta$ , and

$$\Gamma_0 = \frac{G_F^2}{48\pi^3} \frac{\alpha_{\text{em}}^2}{16\pi^2} |V_{tb} V_{ts}^*|^2. \quad (3)$$

In  $\bar{B}^0$  or  $B^-$  [ $B^0$  or  $B^+$ ] decay,  $\theta$  is the angle between the  $\ell^+$  [ $\ell^-$ ] and the  $B$  meson three-momenta in the  $\ell^+ \ell^-$  center-of-mass frame. The Wilson coefficients  $C_{7,9,10}$  contain short-distance information. Beyond tree level they are effectively  $q^2$  dependent and complex, and receive different contributions in inclusive and exclusive decays, as will be discussed below. If there was very precise

data on  $B \rightarrow X_s \ell^+ \ell^-$ , one could extract the individual Wilson coefficients from the  $q^2$  dependence of  $d\Gamma/dq^2$  and the zero of the forward-backward asymmetry. As long as the measurements are limited by experimental uncertainties, it is important to find the most effective ways to extract the short distance information from a few simple observables integrated over  $q^2$ , accessible with limited amount of data.

In Section II we discuss general aspects of an angular decomposition, which gives three observables,  $H_{T,A,L}(q^2)$ . To extract short distance information from these, we separate out the part of the Wilson coefficients sensitive to new physics in a  $q^2$  and  $\mu$  independent manner, and propose to compare measurements of these with their SM predictions. Section III investigates inclusive  $B \rightarrow X_s \ell^+ \ell^-$  decay, while Section IV deals with the exclusive  $B \rightarrow K^* \ell^+ \ell^-$  mode. Section V contains our conclusions. Many analytical results and numerical inputs are collected in the Appendices.

## II. ANGULAR DECOMPOSITION AND DEPENDENCE ON WILSON COEFFICIENTS

The double differential decay rate in  $q^2$  and  $z = \cos\theta$  for either inclusive  $B \rightarrow X_s \ell^+ \ell^-$  or exclusive  $B \rightarrow K^* \ell^+ \ell^-$  decays can be written as

$$\begin{aligned} \frac{d^2\Gamma}{dq^2 dz} &= \frac{3}{8} \left[ (1+z^2) H_T(q^2) + 2z H_A(q^2) \right. \\ &\quad \left. + 2(1-z^2) H_L(q^2) \right]. \end{aligned} \quad (4)$$

The functions  $H_i(q^2)$  are defined to contain the full  $q^2$  dependence of the rate and are independent of  $z$ . They can be extracted from the  $d^2\Gamma/dq^2 dz$  distribution either by a direct fit to the  $z$  dependence or by taking integrals of  $z$ . As special cases we have

$$\begin{aligned} \frac{d\Gamma}{dq^2} &= H_T(q^2) + H_L(q^2), \\ \frac{dA_{\text{FB}}}{dq^2} &= \frac{3}{4} H_A(q^2). \end{aligned} \quad (5)$$

For  $H_L$  the hadronic current is longitudinally polarized, so the rate goes like  $\sin^2 \theta = 1 - z^2$ . For  $H_T$  and  $H_A$  the hadronic current is transversely polarized, with  $H_T$  containing the contributions from purely vector and axial-vector leptonic currents and  $H_A$  containing the interference between vector and axial-vector leptonic currents. In the combinations  $H_T \pm H_A$  the hadronic and leptonic currents have the same (opposite) helicity, giving the usual  $(1 \pm \cos \theta)^2 = (1 \pm z)^2$  dependence. This decomposition is a common tool in the analysis of exclusive semileptonic decays (e.g.,  $B \rightarrow D^* \ell \nu$ ,  $\rho \ell \nu$ ,  $K^* \ell^+ \ell^-$ ) and of decays to two vector mesons (e.g.,  $B \rightarrow \phi K^*$ ,  $J/\psi K^*$ ). In analyzing inclusive  $B \rightarrow X_s \ell^+ \ell^-$ , it should not be harder than measuring  $A_{\text{FB}}$ .

We introduce a scheme to separate certain SM contributions to the rate from terms that are most sensitive to new physics. We define modified Wilson coefficients

$$\begin{aligned} \mathcal{C}_7 &= C_7(\mu) [\overline{m}_b(\mu)/m_b^{1S}] + \dots, \\ \mathcal{C}_9 &= C_9(\mu) + \dots, \\ \mathcal{C}_{10} &\equiv C_{10}. \end{aligned} \quad (6)$$

The ellipses denote a minimal set of perturbative corrections, such that  $\mathcal{C}_{7,9}$  are  $\mu$  independent and real in the SM. These coefficients are given explicitly in Eq. (A2) in Appendix A to  $\mathcal{O}(\alpha_s)$ . The decay rate also depends on SM contributions that are not contained in  $\mathcal{C}_{7,9,10}$ . These are discussed in Secs. III and IV. Of these, the dominant contributions are from the four-quark operators  $O_{1,2}$ , which are expected to be given by the SM. We regard the  $\mathcal{C}_7$ ,  $\mathcal{C}_9$ , and  $\mathcal{C}_{10}$  as the unknown parameters that need to be extracted from experimental data, and compared with the SM or new physics predictions.

We do not expand the  $\overline{\text{MS}}$   $b$ -quark mass,  $\overline{m}_b(\mu)$ , in  $\mathcal{C}_7$ , because it always comes together with  $O_7$  and they should be renormalized together. This also makes the perturbative expansions better behaved. In addition, as indicated in Eq. (6), we use the  $1S$  scheme [9] for all other factors of  $m_b$  (and  $m_c$  as well), which also improves the perturbative expansions. We will drop the superscript  $1S$  hereafter when the distinction is unimportant, but use  $m_b^{1S}$  for  $m_b$  everywhere (except  $\overline{m}_b$ , of course).

At subleading orders in  $\alpha_s$  and  $1/m_b$ , the dependence of the rates on the  $\mathcal{C}_i$ 's will be different in inclusive and exclusive decays. To simplify the explanation of our main points, in the remainder of this section we neglect the contributions from operators other than  $O_{7,9,10}$ . Then, at leading order, the  $H_i$ 's defined in Eq. (4) have the general structure

$$\begin{aligned} H_T(q^2) &\propto 2(1-s)^2 s \left[ \left( \mathcal{C}_9 + \frac{2}{s} \mathcal{C}_7 \right)^2 + \mathcal{C}_{10}^2 \right], \\ H_A(q^2) &\propto -4(1-s)^2 s \mathcal{C}_{10} \left( \mathcal{C}_9 + \frac{2}{s} \mathcal{C}_7 \right), \\ H_L(q^2) &\propto (1-s)^2 \left[ (\mathcal{C}_9 + 2\mathcal{C}_7)^2 + \mathcal{C}_{10}^2 \right]. \end{aligned} \quad (7)$$

Comparing Eqs. (1) and (7) shows that splitting  $d\Gamma/dq^2$  into  $H_L(q^2)$  and  $H_T(q^2)$  separates the contributions with

different  $q^2$  dependences, providing a third independent observable, which has not been studied so far in inclusive  $B \rightarrow X_s \ell^+ \ell^-$ . For exclusive  $B \rightarrow K^* \ell^+ \ell^-$  it is equivalent to the fraction of longitudinal polarization  $F_L = H_L/(H_T + H_L)$  measured by Babar [5].

If one does not resolve the details of the hadronic system, neglects effects proportional to  $m_\ell^2/m_b^2$ , and does not measure the lepton polarization (which might be accessible in  $B \rightarrow X_s \tau^+ \tau^-$  [10], though this is challenging at best), then the only observable linear combinations of the Wilson coefficients are those given in Eq. (7). This is necessarily the case for inclusive  $B \rightarrow X_s e^+ e^-$  and  $B \rightarrow X_s \mu^+ \mu^-$  decays.

In exclusive  $B \rightarrow K^* \ell^+ \ell^-$  decay, if the  $K^* \rightarrow K\pi$  decay is reconstructed, there are two additional observable angles. These are  $\theta_{K^*}$ , which is the analog of  $\theta$  for the  $K\pi$  system, and  $\phi$ , which is the angle between the  $K\pi$  and the  $\ell^+ \ell^-$  planes (using the notation of Babar [5], which follows Ref. [11]). Once one integrates over  $\phi$ , even if the  $\theta$  and  $\theta_{K^*}$  distributions are not integrated over, the rate depends only on the three linear combinations in Eq. (7). Keeping the  $\phi$  dependence would give rise to two further linear combinations [11], and it would require a more detailed study to test whether the measurement could benefit from not integrating over  $\phi$ .

As mentioned above, instead of relying on the full  $q^2$  dependence, we want to integrate over as large regions of  $q^2$  as possible to extract the Wilson coefficients from the simple integrals

$$H_i(q_1^2, q_2^2) = \int_{q_1^2}^{q_2^2} dq^2 H_i(q^2). \quad (8)$$

We restrict our discussion to the low  $q^2$  region,  $1 \text{ GeV}^2 < q_1^2, q_2^2 < 6 \text{ GeV}^2$ , since it is theoretically clean and contains a large part of the rate. The interference of the  $J/\psi$  contribution with the short distance rate is a significant contamination at higher values of  $q^2$ , while the rate for  $q^2 > m_\psi^2 \approx 14.2 \text{ GeV}^2$  is significantly smaller. Ultimately, the measured tail of the long distance contribution will determine the optimal upper cut on  $q^2$ .

For  $H_L(q^2)$  the hadronic current is longitudinally polarized, so the  $\mathcal{C}_7$  contribution is not enhanced by a  $1/s$  pole, and is numerically small. Since the Wilson coefficients in  $H_L$  combine into a  $q^2$  independent overall factor, there is no gain in considering the  $q^2$  dependence of  $H_L(q^2)$ . Thus, to get maximal statistics one should use

$$H_L(1, 6) \propto \mathcal{C}_9^2 + \mathcal{C}_{10}^2 + 4\mathcal{C}_7\mathcal{C}_9 + 4\mathcal{C}_7^2, \quad (9)$$

which is dominated by the  $\mathcal{C}_9^2 + \mathcal{C}_{10}^2$  term.

In contrast, in  $H_T(q^2)$  the different contributions have a hierarchical  $q^2$  dependence, i.e.

$$H_T(q^2) \propto \frac{4}{s} \mathcal{C}_7^2 + 4\mathcal{C}_7\mathcal{C}_9 + s(\mathcal{C}_9^2 + \mathcal{C}_{10}^2). \quad (10)$$

In this case, integrating  $H_T(q^2)$  over  $q^2$ , the  $\mathcal{C}_7\mathcal{C}_9$  interference term in  $H_T(1, 6)$  is as important as the  $\mathcal{C}_9^2 + \mathcal{C}_{10}^2$  contribution, because the latter vanishes for  $q^2 \rightarrow 0$ . Thus,

with enough statistics, it will be worth splitting  $H_T(1, 6)$  into two integrals,  $H_T(1, q_i^2)$  and  $H_T(q_i^2, 6)$ , giving access to two independent combinations of Wilson coefficients. The value of  $q_i^2$  should be chosen to give comparable statistics for the two integrated rates. We will use  $H_T(1, 3.5)$  and  $H_T(3.5, 6)$  below.

Finally,  $H_A(1, 6) \propto A_{\text{FB}}$  has comparable  $\mathcal{C}_7\mathcal{C}_{10}$  and  $\mathcal{C}_9\mathcal{C}_{10}$  contributions. To separate them, one can split  $H_A(1, 6)$  into  $H_A(1, q_i^2)$  and  $H_A(q_i^2, 6)$  similarly to  $H_T$  above, where the precise value of  $q_i^2$  can again vary. We will use  $H_A(1, 3.5)$  and  $H_A(3.5, 6)$ , which give reasonably independent linear combinations of  $\mathcal{C}_7\mathcal{C}_{10}$  and  $\mathcal{C}_9\mathcal{C}_{10}$ . We do not normalize  $H_A(q^2)$  by  $d\Gamma/dq^2$ , as is often done for  $dA_{\text{FB}}/dq^2$ . This would artificially suppress the low  $q^2$  region, without providing any real advantage. If necessary,  $H_A(q^2)$  could be normalized to the rate in a certain  $q^2$  window.

Usually the zero of  $H_A(q^2) \propto dA_{\text{FB}}/dq^2$ , which occurs in the vicinity of  $q_{\text{FB}}^2 = -2m_b^2(\mathcal{C}_7/\mathcal{C}_9)$ , is advocated to determine  $\mathcal{C}_7/\mathcal{C}_9$ . As discussed in the introduction, measuring  $q_{\text{FB}}^2$  requires very large data sets. Measuring two integrals of  $H_A(q^2)$  as described above may be a simpler way to achieve similar sensitivity with less data.

### III. INCLUSIVE $B \rightarrow X_s \ell^+ \ell^-$

In this section we consider the inclusive decay  $B \rightarrow X_s \ell^+ \ell^-$ , working to what is usually referred to as next-to-next-to-leading order (NNLO). We define the effective

coefficients

$$\begin{aligned} \mathcal{C}_7^{\text{incl}}(q^2) &= \mathcal{C}_7 + F_7(q^2) + G_7(q^2), \\ \mathcal{C}_9^{\text{incl}}(q^2) &= \mathcal{C}_9 + F_9(q^2) + G_9(q^2), \end{aligned} \quad (11)$$

such that all terms on the right-hand side of Eq. (11) are separately  $\mu$  independent to the order we are working at.

The functions  $F_i(q^2)$  and  $G_i(q^2)$  are calculated in the SM. The  $F_{7,9}(q^2)$  contain perturbative contributions from the four-quark operators  $O_{1-6}$  and the chromomagnetic penguin operator,  $O_8$ , while the  $G_{7,9}(q^2)$  contain nonperturbative  $\mathcal{O}(1/m_c^2)$  corrections involving the four-quark operators [12]. The latter can be included in a simple form for any differential rate, but the final results have to be reexpanded so that  $\mathcal{O}(\alpha_s/m_c^2, 1/m_c^4)$  terms are not kept. The explicit expressions are given in Appendix A. In the small  $q^2$  region (well below the  $c\bar{c}$  threshold), the  $\mathcal{C}_{7,9}^{\text{incl}}(q^2)$  have only small imaginary parts and modest  $q^2$  dependences, which arise only from  $O_{1-6,8}$  and are fully contained in  $F_i(q^2)$  and  $G_i(q^2)$ . Therefore, all  $\mathcal{C}_i$  are real numbers in the SM, which has the advantage of reducing the number of parameters to three.

At NNLO, we include the corrections to the  $F_i(q^2)$  up to  $\mathcal{O}(\alpha_s)$  where they are known analytically [13, 14, 15, 16], and to the Wilson coefficients of  $O_{1-6,8}$  entering the  $F_i(q^2)$  [17, 18, 19, 20]. At leading order in  $\alpha_s$ ,  $F_7(q^2)$  vanishes, while  $F_9(q^2)$  is nonvanishing. We also include the  $\mathcal{O}(\alpha_s)$  corrections to the matrix elements of  $O_{7,9,10}$  [14, 21, 22] and the nonperturbative  $\mathcal{O}(1/m_b^2)$  [23, 24] corrections. The short distance contributions to the  $H_i(q^2)$  can be written as  $[s = q^2/(m_b^{1S})^2]$

$$\begin{aligned} H_T(q^2) &= 2\Gamma_0(m_b^{1S})^3 (1-s)^2 s \left[ (|\mathcal{C}_9^{\text{incl}}|^2 + \mathcal{C}_{10}^2) h_T^{99}(s) + \frac{4}{s^2} |\mathcal{C}_7^{\text{incl}}|^2 h_T^{77}(s) + \frac{4}{s} \text{Re}(\mathcal{C}_7^{\text{incl}*} \mathcal{C}_9^{\text{incl}}) h_T^{79}(s) \right] + H_T^{\text{brems}}(q^2), \\ H_A(q^2) &= -4\Gamma_0(m_b^{1S})^3 (1-s)^2 s \mathcal{C}_{10} \text{Re} \left[ \mathcal{C}_9^{\text{incl}} h_A^{90}(s) + \frac{2}{s} \mathcal{C}_7^{\text{incl}} h_A^{70}(s) \right] + H_A^{\text{brems}}(q^2), \\ H_L(q^2) &= \Gamma_0(m_b^{1S})^3 (1-s)^2 \left[ (|\mathcal{C}_9^{\text{incl}}|^2 + \mathcal{C}_{10}^2) h_L^{99}(s) + 4|\mathcal{C}_7^{\text{incl}}|^2 h_L^{77}(s) + 4 \text{Re}(\mathcal{C}_7^{\text{incl}*} \mathcal{C}_9^{\text{incl}}) h_L^{79}(s) \right] + H_L^{\text{brems}}(q^2). \end{aligned} \quad (12)$$

The functions  $h_i^j(s)$  are defined to have only a residual  $s$  dependence entering at higher orders in  $\alpha_s$  and  $1/m_b$ , i.e.

$$h_i^j(s) = 1 - 2 \frac{\alpha_s C_F}{4\pi} \omega_i^j(s) + \frac{1}{m_b^2} \chi_i^j(s), \quad (13)$$

with  $C_F = 4/3$ . The  $\omega_i^j(s)$  and  $\chi_i^j(s)$  containing the  $\mathcal{O}(\alpha_s)$  and  $\mathcal{O}(1/m_b^2)$  corrections are given in Appendix A. We neglect the finite bremsstrahlung corrections due to four-quark operators,  $H_i^{\text{brems}}(q^2)$ , which are not known for the double differential rate  $d^2\Gamma/dq^2 dz$ . This should be a safe approximation, since in the known cases of  $d\Gamma/dq^2$  [25] and  $dA_{\text{FB}}/dq^2$  [26] they are at or below the one percent level.

To make numerical predictions we use the input values collected in Appendix B. Since the value of  $m_b^{1S}$  is known to better than one percent, there is no benefit in normalizing the rates to  $\Gamma(B \rightarrow X \ell \bar{\nu})$ . We find

$$\begin{aligned} H_T(1, 3.5)/\Gamma_0 &= 37.18 (\mathcal{C}_9^2 + \mathcal{C}_{10}^2) + 15550. \mathcal{C}_7^2 + 1409. \mathcal{C}_7 \mathcal{C}_9 - 119.4 \mathcal{C}_9 - 2795. \mathcal{C}_7 - 69.65, \\ H_T(3.5, 6)/\Gamma_0 &= 59.76 (\mathcal{C}_9^2 + \mathcal{C}_{10}^2) + 1067. \mathcal{C}_7 \mathcal{C}_9 + 5008. \mathcal{C}_7^2 - 76.25 \mathcal{C}_9 - 778.2 \mathcal{C}_7 - 67.72, \\ H_A(1, 3.5)/\Gamma_0 &= -\mathcal{C}_{10} (70.19 \mathcal{C}_9 + 1401. \mathcal{C}_7 - 121.5), \\ H_A(3.5, 6)/\Gamma_0 &= -\mathcal{C}_{10} (111.8 \mathcal{C}_9 + 1051. \mathcal{C}_7 - 80.91), \\ H_L(1, 6)/\Gamma_0 &= 315.2 (\mathcal{C}_9^2 + \mathcal{C}_{10}^2) + 1377. \mathcal{C}_7^2 + 1299. \mathcal{C}_7 \mathcal{C}_9 + 33.41 \mathcal{C}_9 + 86.86 \mathcal{C}_7 - 72.87. \end{aligned} \quad (14)$$

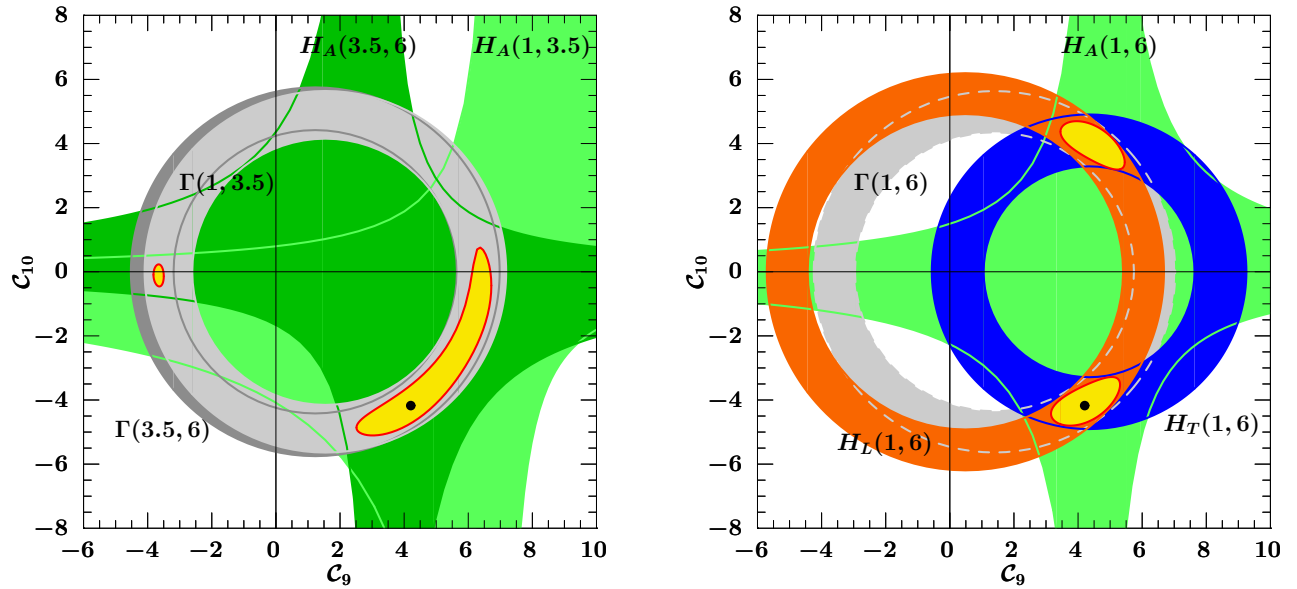


FIG. 1: (color online) Constraints in the  $C_9$ – $C_{10}$  plane. Left:  $\Gamma(1, 3.5)$  and  $\Gamma(3.5, 6)$  [light and medium (gray) annuli],  $H_A(1, 3.5)$  and  $H_A(3.5, 6)$  [light and dark (green) regions bounded by hyperbolae]. Right:  $H_T(1, 6)$  [dark (blue) annulus],  $H_L(1, 6)$  [medium (orange) annulus],  $H_A(1, 6)$  [light (green) region bounded by hyperbolae], and for comparison  $\Gamma(1, 6)$  [light (gray) annulus]. The black dots show the assumed (SM) central values. The combined constraints are also shown [small light (yellow) regions].

The major uncertainties in Eqs. (14) arise from higher order perturbative corrections,  $m_b$  and  $m_c$ . Varying the renormalization scale between  $m_b/2$  and  $2m_b$ , we get less than 5% uncertainty in the coefficients of the dominant terms in Eq. (14). Since the difference  $m_b - m_c$  is known precisely [27], we vary  $m_b$  and  $m_c$  in a correlated manner, which gives a 1–5% uncertainty. The uncertainties from other input parameters and higher order corrections in  $1/m_b$  are much smaller. The uncertainties from the electroweak matching scale,  $\mu_0$ , and the top-quark mass,  $m_t$ , in Eq. (14) are negligible, because they primarily enter via the values of the  $C_i$ . Using Eq. (14) and the SM values of  $C_i$  from Table I, we obtain the SM prediction for the  $B \rightarrow X_s \ell^+ \ell^-$  branching ratio for  $1 \text{ GeV}^2 < q^2 < 6 \text{ GeV}^2$ ,

$$\tau_B \Gamma(1, 6) = (1.575 \pm 0.067_{[\mu]} \pm 0.051_{[m_b, m_c]} \pm 0.041_{[m_t]} \pm 0.019_{[\mu_0]}) \times 10^{-6}. \quad (15)$$

This agrees well with Refs. [16, 20] and with Ref. [28], which also uses the  $1S$  scheme.

To estimate the future uncertainties, we scale the current measurements [2, 3] to  $1 \text{ ab}^{-1}$  luminosity, which gives about 10% statistical uncertainty for  $\Gamma(1, 6)$ . We assume that the  $H_i$  are measured with the central values given by the SM. The statistical error of  $H_T$  and  $H_L$  is obtained by scaling by the number of events compared to  $\Gamma(1, 6)$ . In the case of  $H_A$  we take the same absolute statistical error for  $3/4 H_A$  as for the total rate integrated over the same  $q^2$ -region. The reason is that  $3/4 H_A$  corresponds to the difference between the rates for positive and negative  $\cos \theta$ , which has the same absolute statistical error as the sum. To this we add in quadrature

a 20% systematic uncertainty for all  $H_i$ , to account for experimental systematics and theoretical uncertainties. From each observable's total error we build  $\chi^2$  for the individual and combined constraints, and Figs. 1 and 2 show the  $\Delta\chi^2 = 1$  regions in the  $C_9$ – $C_{10}$  plane. Since  $B \rightarrow X_s \gamma$  will always be measured with higher precision than  $B \rightarrow X_s \ell^+ \ell^-$ , we consider the value of  $C_7^2$  to be known from  $B \rightarrow X_s \gamma$  and assume its sign is negative as in the SM (since there is an overall sign ambiguity).

On the left-hand side in Fig. 1 we show the constraints from  $\Gamma(1, 3.5)$ ,  $\Gamma(3.5, 6)$  [light and medium (gray) annuli],  $H_A(1, 3.5)$ , and  $H_A(3.5, 6)$  [light and dark (green) regions bounded by hyperbolae]. This plot shows that splitting  $\Gamma(1, 6)$  into two regions is not really useful because a very similar linear combination of Wilson coefficients is constrained. As is well known, splitting  $H_A(1, 6)$  into two regions is very useful, since different combinations of coefficients are constrained by each region. (This is also the reason why the zero of the forward-backward asymmetry is interesting to study.) The plot on the right in Fig. 1 shows that splitting  $\Gamma(1, 6)$  into  $H_T(1, 6)$  [dark (blue) annulus] and  $H_L(1, 6)$  [medium (orange) annulus] gives a very powerful constraint. This shows the power of separately measuring  $H_T$  and  $H_L$  as advocated in the introduction. The observables shown in this figure are sufficient to extract the absolute values  $|C_i|$  and the sign of  $C_9$  relative to  $C_7$ . The constraint from  $\Gamma(1, 6)$  is also plotted [light (gray) annulus], which shows that separating  $\Gamma$  into  $H_T$  and  $H_L$  significantly improves the constraints. However, because of its large relative error,  $H_A(1, 6)$  [light (green) region bounded by hyperbolae] does not provide

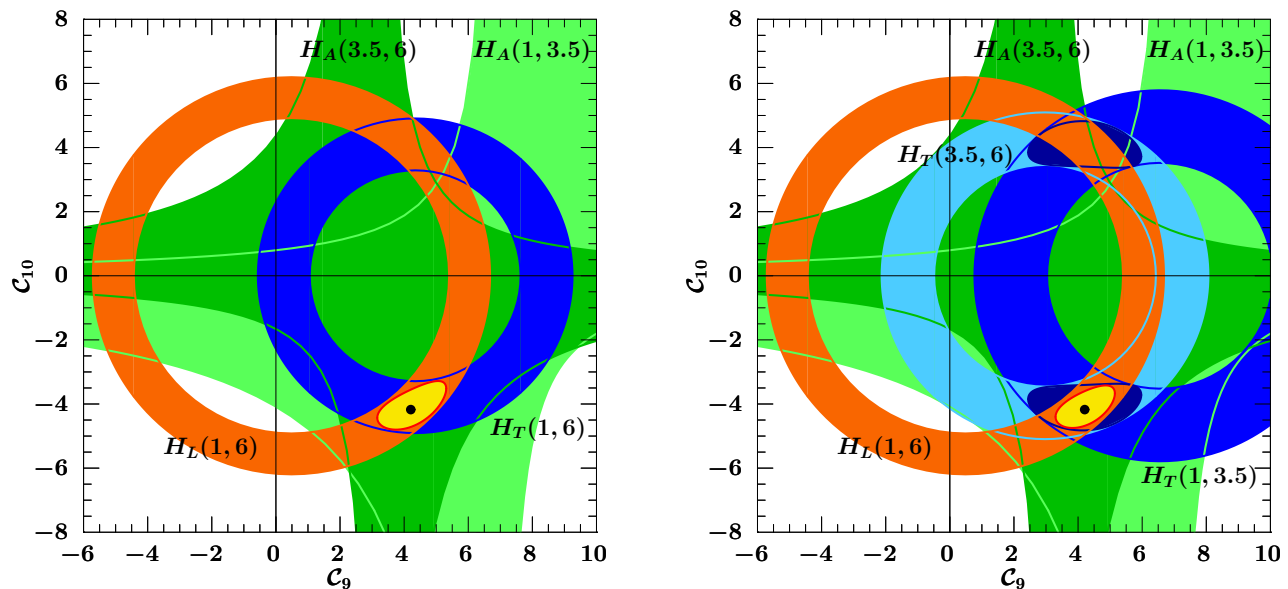


FIG. 2: (color online) Constraints in the  $C_9 - C_{10}$  plane. Left:  $H_T(1,6)$  [dark (blue) annulus],  $H_L(1,6)$  [medium (orange) annulus],  $H_A(1,3.5)$  and  $H_A(3.5,6)$  [light and dark (green) regions bounded by hyperbolae]. Right: as on the left, but  $H_T$  split into  $H_T(1,3.5)$  and  $H_T(3.5,6)$  [dark and light (blue) annuli]. The right plot also shows the constraint from the two  $H_T$  observables alone [small black (dark blue) regions]. All other notations are as in Fig 1.

a good constraint.

The left plot in Fig. 2 shows that splitting  $H_A$  into two regions gives sensitivity to the sign of  $C_{10}$ . Measuring  $H_A(1,3.5)$  and  $H_A(3.5,6)$  can distinguish between the positive and negative solutions for  $C_{10}$ . Combined with the tighter constraints from splitting  $\Gamma$  into  $H_T$  and  $H_L$ , splitting of  $H_A$  into these two regions gives similar information as the zero of  $A_{FB}$ . The plot on the right in Fig. 2 shows that splitting  $H_T(1,6)$  into  $H_T(1,3.5)$  and  $H_T(3.5,6)$  can further overconstrain the determination of the Wilson coefficients. The black (dark blue) region in the right plot in Fig. 2 shows the combined constraint from only the two  $H_T$  integrals. The requirement that the  $H_L$  constraint overlaps with it effectively provides a consistency test on the value of  $C_7$  extracted from  $B \rightarrow X_s \gamma$ . It can also play an important role in the search for physics beyond the SM. If the new physics introduces low energy operators with a helicity structure different from the SM, it will affect  $H_L$  and  $H_T$  differently, because of their different polarizations.

It would also be interesting to explore experimentally whether the influence of the  $J/\psi$  resonance turns on at similar  $q^2$  values in  $H_T$ ,  $H_A$ , and  $H_L$ . Since we have no information on the  $J/\psi$  polarization in inclusive  $B \rightarrow J/\psi X_s$  decay, it is possible that the upper cut on  $q^2$  can be extended past  $6 \text{ GeV}^2$  in some (but maybe not all) of these observables, which may improve the statistical accuracy of the measurement.

#### IV. EXCLUSIVE $B \rightarrow K^* \ell^+ \ell^-$

We now turn to the exclusive decay  $B \rightarrow K^* \ell^+ \ell^-$ . While the theoretical uncertainties are larger than in the inclusive analysis, measuring the exclusive mode is simpler and it may be the only possibility at LHCb. Compared with the inclusive decay, the exclusive measurements go closer to  $q^2 = m_\psi^2$ :  $8.1 \text{ GeV}^2$  at Belle [4] and  $8.4 \text{ GeV}^2$  at Babar [5]. In this region of phase space the energy of the  $K^*$  varies only between  $1.9 \text{ GeV} < E_{K^*} < 2.7 \text{ GeV}$ , which helps control some theoretical uncertainties. In our general discussion we will consider for simplicity  $0.1 \text{ GeV}^2 < q^2 < 8 \text{ GeV}^2$ , where the precise value of neither limit is important (the lower limit can be replaced by any experimentally appropriate value above  $4m_\ell^2$ ). However, for comparisons of our results with the data, we use the limits used in the experimental analysis.

In this section we explain that, similarly to the inclusive decay, all the information obtainable can be extracted from a few integrated rates. To obtain the most information on the ratios of Wilson coefficients, Belle [4] performed a maximum-likelihood fit to the double differential distribution  $d^2\Gamma/dq^2 dz$ . However, since the theoretical predictions change for the double differential rate as they are being refined, we think that a few integrated rates will be very useful to compare the theory with the data. In addition, results from different experiments are more straightforward to combine for these partial rates.

In the heavy quark limit, soft-collinear effective theory (SCET) [29] relates the seven full QCD form factors that describe  $B \rightarrow K^* \ell^+ \ell^-$  to fewer functions. We follow the notation of Ref. [30], and denote these by  $\zeta_{\perp,\parallel}$  and

$\zeta_{\perp,\parallel}^J$ . The  $\zeta_{\perp,\parallel}$  obey the form factor relations [31], while  $\zeta_{\perp,\parallel}^J$  violate them. Whether  $\zeta^J/\zeta$  is  $\mathcal{O}(\alpha_s)$  or  $\mathcal{O}(1)$  is subject to discussion, and so at the present time the  $\alpha_s$

corrections in exclusive decay are not fully known.

The angular decomposition for  $B \rightarrow K^* \ell^+ \ell^-$  is [15, 32, 33]

$$\begin{aligned} H_T(q^2) &= 2\Gamma_0 m_B^3 \lambda^3 s \left\{ \mathcal{C}_{10}^2 [\zeta_{\perp}(s)]^2 + \left| C_9^{\text{excl}} \zeta_{\perp}(s) + \frac{2C_7^{\text{excl}}}{s} \frac{m_b^{1S}}{m_B} [\zeta_{\perp}(s) + (1-s) \zeta_{\perp}^J(s)] \right|^2 \right\}, \\ H_A(q^2) &= -4\Gamma_0 m_B^3 \lambda^3 s \mathcal{C}_{10} \zeta_{\perp}(s) \left\{ C_9^{\text{excl}} \zeta_{\perp}(s) + \frac{2C_7^{\text{excl}}}{s} \frac{m_b^{1S}}{m_B} [\zeta_{\perp}(s) + (1-s) \zeta_{\perp}^J(s)] \right\}, \\ H_L(q^2) &= \frac{1}{2} \Gamma_0 m_B^3 \lambda^3 \left( \mathcal{C}_{10}^2 + \left| C_9^{\text{excl}} + 2C_7^{\text{excl}} \frac{m_b^{1S}}{m_B} \right|^2 \right) [\zeta_{\parallel}(s) - \zeta_{\parallel}^J(s)]^2. \end{aligned} \quad (16)$$

In this section  $s = q^2/m_B^2$ . In Eq. (16),  $\rho = m_{K^*}^2/m_B^2 \sim 0.03$  and  $\lambda = [(1-s)^2 - 2\rho(1+s) + \rho^2]^{1/2}$ . In analogy to Eq. (11), we have defined

$$\begin{aligned} \mathcal{C}_7^{\text{excl}}(q^2) &= \mathcal{C}_7 + F_7(q^2) + \mathcal{O}(\alpha_s), \\ \mathcal{C}_9^{\text{excl}}(q^2) &= \mathcal{C}_9 + F_9(q^2) + \mathcal{O}(\alpha_s). \end{aligned} \quad (17)$$

Note that there are additional  $\mathcal{O}(\alpha_s)$  corrections beyond  $F_{7,9}(q^2)$  [15, 34], and we do not attempt to address power suppressed terms.

Without lattice QCD (LQCD) input, model calculations, or nonleptonic decay data to constrain  $\zeta_{\parallel}^{(J)}$ , we cannot learn about the  $\mathcal{C}_i$ 's from  $H_L$ . However, the magnitudes of the form factors  $\zeta_{\perp}^{(J)}$  can be constrained from the  $B \rightarrow K^* \gamma$  rate,

$$\begin{aligned} \Gamma(B \rightarrow K^* \gamma) &= \frac{G_F^2}{8\pi^3} \frac{\alpha_{\text{em}}}{4\pi} |V_{tb} V_{ts}^*|^2 m_B^3 (m_b^{1S})^2 (1-\rho)^3 \\ &\quad \times |\mathcal{C}_7^{\text{excl}}(0)|^2 [\zeta_{\perp}(0) + \zeta_{\perp}^J(0)]^2. \end{aligned} \quad (18)$$

In Eqs. (18), (16), and (22) we display the kinematical  $\rho$  dependences, but neglect the “dynamical” ones, which would, for example, multiply  $\zeta_{\perp}^J(0)$  in Eq. (18) by  $(1-\rho)$ .

The  $\zeta$  and  $\zeta^J$  form factors are functions of the  $K^*$  energy,  $E_{K^*} = (m_B/2)(1-s+\rho)$ . In the heavy quark limit, a convenient parameterization is

$$\zeta_{\perp}^{(J)}(s) = \frac{\zeta_{\perp}^{(J)}(0)}{(1-s)^2} [1 + \mathcal{O}(\alpha_s, \Lambda/E_{K^*})], \quad (19)$$

i.e., the form factors' leading  $E$  dependence is  $1/E_{K^*}^2$ . Since in the  $0.1 \text{ GeV}^2 < q^2 < 8.4 \text{ GeV}^2$  region  $E_{K^*}$  varies only over  $1.9 \text{ GeV} < E_{K^*} < 2.7 \text{ GeV}$ , we do not expect large deviations from this limit. For example,  $\zeta_{\perp}$  can have additional logarithmic dependence on  $E_{K^*}$  [35], which is roughly constant over this small region.

In the literature  $\zeta^J/\zeta$  is often treated as  $\mathcal{O}(\alpha_s)$ . The zero-bin [36] shows that this is not the case parametrically, so we treat both  $\zeta_{\perp}(0)$  and  $\zeta_{\perp}^J(0)$  as independent nonperturbative parameters, and neglect  $\mathcal{O}(\alpha_s)$  corrections to  $\zeta_{\perp}^{(J)}(s)$ , which are partially known. These same

considerations also imply that the zero of the forward-backward asymmetry in  $B \rightarrow K^* \ell^+ \ell^-$ ,  $q_{\text{FB}}^2$ , does not necessarily provide as precise and as model independent a determination of  $\mathcal{C}_7/\mathcal{C}_9$  as claimed in much of the literature. Moreover, even after 5 years of LHCb data taking ( $10 \text{ fb}^{-1}$ ), one expects  $\sigma(q_{\text{FB}}^2) \approx 0.5 \text{ GeV}^2$ , which would determine  $\mathcal{C}_7/\mathcal{C}_9$  only with an approximately 13% error in the SM [37].

Some of the known  $\mathcal{O}(\alpha_s)$  corrections to Eqs. (16) and (18) can be included in Eq. (17). However, since we treat  $\zeta_{\perp}(0)$  and  $\zeta_{\perp}^J(0)$  as independent unknowns and determine them from the data, only the part of the  $\alpha_s$  corrections that causes these form factors to deviate from their asymptotic  $s$  dependences in Eq. (19) will introduce errors. Since in the  $0.1 \text{ GeV}^2 < q^2 < 8 \text{ GeV}^2$  region that we concentrate on,  $0 < s < 0.3$ , we expect that the neglected  $\mathcal{O}(\alpha_s)$  terms do not introduce a dominant error. Moreover, they could be added to our analysis.

From the ratios of the four observables

$$\Gamma(B \rightarrow K^* \gamma), \quad H_T(0.1, 8), \quad H_A(0.1, 4), \quad H_A(4, 8), \quad (20)$$

one can extract

$$\frac{\mathcal{C}_9}{\mathcal{C}_7}, \quad \frac{\mathcal{C}_{10}}{\mathcal{C}_7}, \quad r = \frac{\zeta_{\perp}^J(0)}{\zeta_{\perp}(0) + \zeta_{\perp}^J(0)}. \quad (21)$$

If one does not want to use the  $B \rightarrow K^* \gamma$  data then ratios of  $H_T(0.1, 4)$ ,  $H_T(4, 8)$ ,  $H_A(0.1, 4)$ , and  $H_A(4, 8)$  could also be used. The ratio  $r$  is of great interest for heavy quark theory. One expects  $r$  to be roughly similar in size as the same ratio involving the  $\zeta_{\parallel}^{(J)}$  form factors, which enters the determination of the unitarity triangle angle  $\gamma$  (or  $\alpha$ ) from charmless two-body  $B$  decays.

At present there is insufficient published data to carry out this analysis to determine the Wilson coefficients. However,  $\Gamma(B \rightarrow K^* \gamma)$  is well measured [38] and  $H_T(0.1, 8.4)$  can be obtained from the Babar measurement [5]. (Belle [4] does a maximum-likelihood fit to extract information on the Wilson coefficients, so we cannot use their fit result projected on to the forward-backward

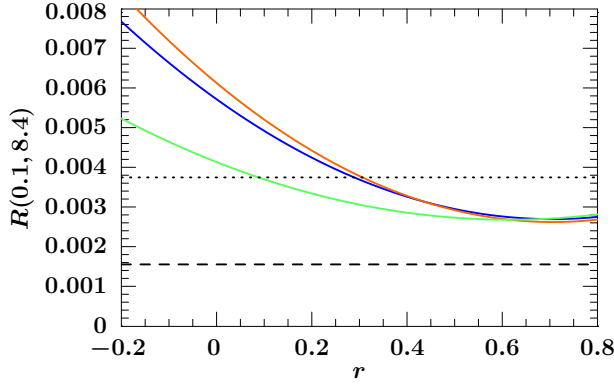


FIG. 3: (color online) The ratio  $R(0.1, 8.4)$  defined in Eq. (22) as a function of  $r$  [dark (blue) curve], assuming the SM values for all  $C_i$ . The medium (orange) curve includes the  $\mathcal{O}(1)$  correction from  $F_9(q^2)$ , and the light (green) curve in addition includes  $\mathcal{O}(\alpha_s)$  corrections from  $F_{7,9}(q^2)$  in Eq. (17). The dashed [dotted] line shows the central value [ $1\sigma$  upper bound] from the Babar measurement [5].

asymmetry as a direct measurement of  $H_A$  in the corresponding bins.) Assuming the SM for  $C_{7,9,10}$ , we can use  $\Gamma(B \rightarrow K^*\gamma)$  and  $H_T(0.1, 8.4)$  to constrain  $r$ . The ratio

$$R(q_1^2, q_2^2) \equiv \frac{H_T(q_1^2, q_2^2)}{\Gamma(B \rightarrow K^*\gamma)} = \frac{\alpha_{\text{em}}}{12\pi} \frac{m_B^2}{(m_b^{1S})^2} \int_{q_1^2/m_B^2}^{q_2^2/m_B^2} ds \frac{\lambda^3 s}{(1-\rho)^3 (1-s)^4} \times \left\{ \frac{C_{10}^2}{C_7^2} (1-r)^2 + \left[ \frac{C_9}{C_7} (1-r) + \frac{2}{s} \frac{m_b^{1S}}{m_B} (1-sr) \right]^2 \right\}, \quad (22)$$

as a function of  $r$  is shown in Fig. 3 for  $R(0.1, 8.4)$ . The dark (blue) curve shows Eq. (22), the medium (orange) one includes the leading corrections to  $C_9^{\text{excl}}(q^2)$  from  $F_9(q^2)$ , and the light (green) curve includes in addition the  $\mathcal{O}(\alpha_s)$  corrections from  $F_{7,9}(q^2)$ . The significant change is dominantly due to the large  $F_7(0)$  contribution to  $C_7^{\text{excl}}(0)$ , also observed for  $\Gamma(B \rightarrow K^*\gamma)$  [15, 39]. This shows that a complete understanding of the  $\alpha_s \zeta_i^J$  corrections to these exclusive decays is very important. Until this is achieved, a determination of  $C_9/C_7$ ,  $C_{10}/C_7$ , and  $r$  without the  $\Gamma(B \rightarrow K^*\gamma)$  data, using only two bins of each  $H_T$  and  $H_A$ , as mentioned after Eq. (21), may be theoretically cleaner.

The central value,  $R(0.1, 8.4) = 1.55 \times 10^{-3}$  [5], and the  $1\sigma$  upper bound are shown in Fig. 3 by dashed and dotted lines, respectively. Since the error is still large, at the moment one cannot make a statistically significant statement about the size of  $r$ . Nevertheless, we expect that (if the SM is valid) the central value of  $R(0.1, 8.4)$  should go up, probably via an increase in the transverse polarization fraction in this  $q^2$  region.

Until precise unquenched LQCD calculations of the  $B \rightarrow K^{(*)}$  form factors for small  $q^2$  become available, the method outlined above may provide the most accu-

rate extraction of short distance information from  $B \rightarrow K^*\ell^+\ell^-$ . With more statistics in the future it should become possible to determine the quantities in Eq. (21), providing new tests of the SM and insights into the theory of hadronic  $B$  decays.

We did not consider  $B \rightarrow K\ell^+\ell^-$  decay, because  $B \rightarrow K\gamma$  is forbidden by angular momentum conservation, so it is not possible to learn about the short distance physics from this mode without using a determination of the corresponding form factors from lattice QCD or model calculations. (This is similar to the case of  $H_L^{B \rightarrow K^*\ell^+\ell^-}$  explained above.) To proceed by using model independent continuum methods, one would have to use  $B \rightarrow \pi\ell\bar{\nu}$  data combined with  $SU(3)$  flavor symmetry or the two-body charmless nonleptonic decay data to constrain the  $B \rightarrow K$  form factor.

## V. CONCLUSIONS

In this paper we pointed out that in inclusive  $B \rightarrow X_s\ell^+\ell^-$  decay an angular decomposition provides a third  $q^2$  dependent observable in addition to the total rate and the forward-backward asymmetry. Splitting up the rate into transverse and longitudinal parts, proportional to  $1 + \cos^2\theta$  ( $H_T$ ) and  $1 - \cos^2\theta$  ( $H_L$ ), one gains access to a third independent linear combination of Wilson coefficients. This requires measuring no additional kinematical variable besides  $q^2$  and  $\cos\theta$ , which are already studied by Babar and Belle. Without doing more complicated analyses, it will improve the determination of the relevant Wilson coefficients and the sensitivity to possible non-SM physics.

To incorporate the existing NNLO calculations, we proposed a new scheme that defines  $q^2$  independent coefficients,  $C_7$  and  $C_9$ , which are real in the SM. The  $C_{7,9}$  do not contain certain SM contributions (involving  $C_{1-6,8}$ ), which make the coefficients usually referred to in the literature as  $C_{7,9}^{\text{eff}}$  complex and  $q^2$  dependent. We view  $C_7$ ,  $C_9$ , and  $C_{10} \equiv C_{10}$  as the unknowns sensitive to physics beyond the SM to be extracted from data.

Since precise measurements of the  $q^2$  dependences require very large data sets, we studied how one can extract all Wilson coefficients obtainable from  $B \rightarrow X_s\ell^+\ell^-$  from a few simple integrals of the  $H_{T,L,A}$  components of the decay rate. We concentrated on the low  $q^2$  region ( $1 \text{ GeV}^2 < q^2 < 6 \text{ GeV}^2$ ) and found (see Figs. 1 and 2) that splitting the total rate into transverse and longitudinal parts is a powerful tool to gain more information.

The same angular decomposition in exclusive  $B \rightarrow K^*\ell^+\ell^-$  decay, together with the well-measured  $B \rightarrow K^*\gamma$  rate, also provides a determination of the Wilson coefficients, without reliance on form factor models and without requiring a measurement of the zero of the forward-backward asymmetry. In the heavy quark limit, as a starting point of a systematic expansion, one can parameterize the form factors in the low  $q^2$  region by just a few numbers [see Eq. (19)]. Measuring the observ-



ables in Eq. (20), one can extract from the data both the hadronic unknowns and the Wilson coefficients. A more complete understanding of the  $B \rightarrow K^* \ell^+ \ell^-$  decay may be expected in the near future and will help to firm up the error estimates in such an analysis based on the  $B \rightarrow K^* \ell^+ \ell^-$  data.

It is not known if a truly inclusive study of  $B \rightarrow X_d \ell^+ \ell^-$  will ever be feasible experimentally, but it may be possible to study the exclusive decay  $B \rightarrow \rho \ell^+ \ell^-$ . The methods discussed in this paper are clearly applicable to these decays as well.

With significantly more data, one may prefer to split the rate into more than two bins in the  $1 \text{ GeV}^2 < q^2 < 6 \text{ GeV}^2$  region. One can then search for non-SM physics by fitting for complex  $\mathcal{C}_{7,9,10}$  values, or allowing opposite chirality operators absent in the SM (model independently there is no preference which way to extend the parameter space). Given the good overall consistency of the SM, overconstraining determinations of the Wilson coefficients, such as that in Fig. 2b, may give the best sensitivity to new physics (similarly to the CKM fit).

We did not include shape function effects [40] in our analysis for the inclusive decay (nor are they included in any other paper performing fits to extract short distance physics from the low  $q^2$  region). This is left for future work. Based on Ref. [40], we anticipate that if the  $B \rightarrow X_s \gamma$  photon spectrum is used to understand the effect of the  $m_X$  cut in  $B \rightarrow X_s \ell^+ \ell^-$ , then the analysis considered in this paper will receive only modest corrections, leaving the general picture of how best to extract the Wilson coefficients unchanged.

### Acknowledgments

We are grateful to Peter Cooper, Enrico Lunghi and especially Jeff Berryhill for helpful conversations. We thank Christoph Bobeth for providing us with his Mathematica code for the running of the Wilson coefficients as given in Refs. [19, 20]. Z.L. thanks the MIT CTP for its hospitality while part of this work was completed. This work was supported in part by the Director, Office

of Science, Offices of High Energy and Nuclear Physics of the U.S. Department of Energy under the Contracts DE-AC02-05CH11231 (Z.L. and F.T.), and the cooperative research agreement DOE-FC02-94ER40818 (I.S.). I.S. was also supported in part by the DOE OJI program and by the Sloan Foundation.

### APPENDIX A: ANALYTICAL RESULTS

Here we collect the explicit results for all  $\alpha_s$  and power corrections used in the main text. The Wilson coefficients  $C_i(\mu)$  refer to the operator basis of Refs. [18, 19], except that we keep  $C_{7-10}$  in the traditional normalization [41]. Their numerical values are collected in Table I below. (The corresponding coefficients in the normalization of Ref. [19] are  $\alpha_s/(4\pi)C_{7-10}$ .) Since the formally leading term in  $C_9(m_b)$  is numerically small, it is often considered as  $\mathcal{O}(1)$  in the recent literature. In our case this is not an issue because we treat  $C_9$  as an unknown  $\mathcal{O}(1)$  parameter to be extracted from experiment.

Throughout this paper we work in the  $1S$  scheme [9], with  $m_{c,b}$  always referring to the  $1S$  masses  $m_{c,b}^{1S}$ . They are related to the pole masses,  $m^{\text{pole}}$ , by ( $C_F = 4/3$ )

$$m^{1S} = m^{\text{pole}} \left[ 1 - \frac{\alpha_s(\mu) C_F}{4\pi} \delta^{1S}(\mu) + \mathcal{O}(\alpha_s^2 \delta^{1S}) \right], \quad (\text{A1})$$

where  $\delta^{1S}(\mu) = (\pi/2)\alpha_s(\mu)C_F$  is formally counted as  $\mathcal{O}(1)$ . By definition  $m^{1S}$  is  $\mu$  independent. The  $\mu$  dependence reenters when the perturbative expansion on the right-hand side of Eq. (A1) is truncated. Switching from the pole to the  $1S$  scheme, one reexpands the perturbative expressions to a given order in  $\alpha_s$ , counting  $\delta^{1S} \sim \mathcal{O}(1)$ , and using the same scale  $\mu$  in Eq. (A1) as everywhere else. All perturbative expressions below have been converted to the  $1S$  scheme. The expressions in the pole scheme given in the literature are recovered by setting  $\delta^{1S}(\mu) = 0$  and  $m_b^{1S} = m_b^{\text{pole}}$  everywhere.

In the following, repeated indices are summed from 1 to 6. The coefficients  $\mathcal{C}_{7-10}$  in Eq. (11) are defined as

$$\begin{aligned} \mathcal{C}_7 &= C_7(\mu) \frac{\overline{m}_b(\mu)}{m_b^{1S}} + C_i(\mu) \kappa_{i7} - \frac{\alpha_s(\mu)}{4\pi} \ln \frac{\mu}{m_b^{1S}} \left[ \frac{8}{3} C_7(\mu) \frac{\overline{m}_b(\mu)}{m_b^{1S}} - \frac{32}{9} C_8(\mu) + C_i(\mu) \left( \gamma_{ij}^{(0)} \kappa_{j7} + \gamma_{i7}^{(0)} \right) \right] + \mathcal{O}(\alpha_s^2), \\ \mathcal{C}_8 &= C_8(\mu) + C_i(\mu) \kappa_{i8} + \mathcal{O}(\alpha_s), \\ \mathcal{C}_9 &= C_9(\mu) + C_i(\mu) \left[ \kappa_{i9} - \gamma_{i9}^{(-1)} \ln \frac{\mu}{m_b^{1S}} - \frac{\alpha_s(\mu)}{4\pi} \ln \frac{\mu}{m_b^{1S}} \left( \gamma_{ij}^{(0)} \kappa_{j9} + \gamma_{i9}^{(0)} - \frac{1}{2} \gamma_{ij}^{(0)} \gamma_{j9}^{(-1)} \ln \frac{\mu}{m_b^{1S}} \right) \right] + \mathcal{O}(\alpha_s^2), \\ \mathcal{C}_{10} &= C_{10}, \end{aligned} \quad (\text{A2})$$

where the higher order  $\alpha_s$  corrections are determined by the requirements that they vanish at  $\mu = m_b^{1S}$  and that the  $C_i$  are  $\mu$  independent to a given order. For convenience we also defined  $\mathcal{C}_8$ . It enters the  $F_i(q^2)$  (see below) at  $\mathcal{O}(\alpha_s)$ ,



so we need it only at lowest order. The relevant entries of the anomalous dimension matrices are [13, 18, 19]

$$\gamma_{ij}^{(0)} = \begin{pmatrix} -4 & \frac{8}{3} & 0 & -\frac{2}{9} & 0 & 0 \\ 12 & 0 & 0 & \frac{4}{3} & 0 & 0 \\ 0 & 0 & 0 & -\frac{52}{3} & 0 & 2 \\ 0 & 0 & -\frac{40}{9} & -\frac{100}{9} & \frac{4}{9} & \frac{5}{6} \\ 0 & 0 & 0 & -\frac{256}{3} & 0 & 20 \\ 0 & 0 & -\frac{256}{9} & \frac{56}{9} & \frac{40}{9} & -\frac{2}{3} \end{pmatrix}, \quad \begin{aligned} \gamma_{i7}^{(0)} &= \left( -\frac{232}{243}, \frac{464}{81}, \frac{64}{81}, -\frac{200}{243}, -\frac{6464}{81}, -\frac{11408}{243} \right), \\ \gamma_{i9}^{(-1)} &= \left( -\frac{32}{27}, -\frac{8}{9}, -\frac{16}{9}, \frac{32}{27}, -\frac{112}{9}, \frac{512}{27} \right), \\ \gamma_{i9}^{(0)} &= \left( -\frac{2272}{729}, \frac{1952}{243}, -\frac{6752}{243}, -\frac{2192}{729}, -\frac{84032}{243}, -\frac{37856}{729} \right). \end{aligned} \quad (\text{A3})$$

The constants  $\kappa_{ij}$  in Eqs. (A2) are included by convention to make the leading order contributions to the  $\mathcal{C}_i$  renormalization scheme independent, and are given by [18, 19]

$$\kappa_{i7} = \left( 0, 0, -\frac{1}{3}, -\frac{4}{9}, -\frac{20}{3}, -\frac{80}{9} \right), \quad \kappa_{i8} = \left( 0, 0, 1, -\frac{1}{6}, 20, -\frac{10}{3} \right), \quad \kappa_{i9} = \left( 0, 0, 0, \frac{4}{3}, \frac{64}{9}, \frac{64}{27} \right). \quad (\text{A4})$$

The functions  $F_i(q^2)$  in Eq. (11) contain perturbative corrections arising from  $O_{1-6,8}$ . To  $\mathcal{O}(\alpha_s)$ ,

$$\begin{aligned} F_7(q^2) &= -\frac{\alpha_s(\mu)}{4\pi} \left[ C_i(\mu) f_i^{(7)}(\hat{m}_c, s) + \mathcal{C}_8 f_8^{(7)}(s) \right], \\ F_9(q^2) &= C_i(\mu) \left[ \delta_{ij} - \frac{\alpha_s(\mu)}{4\pi} \ln \frac{\mu}{m_b^{1S}} \gamma_{ij}^{(0)} \right] [t_j h(\hat{m}_c, s) + u_j h(1, s) + w_j h(0, s)] - \frac{\alpha_s(\mu)}{4\pi} [C_i(\mu) f_i^{(9)}(\hat{m}_c, s) + \mathcal{C}_8 f_8^{(9)}(s)] \\ &\quad - \frac{\alpha_s(\mu)}{4\pi} \frac{16}{9} \delta^{1S}(\mu) C_i(\mu) \left[ t_i \frac{\mathcal{F}[s/(4\hat{m}_c^2)]}{1-s/(4\hat{m}_c^2)} + u_i \frac{\mathcal{F}(s/4)}{1-s/4} - \frac{2}{3}(t_i + u_i + w_i) \right], \end{aligned} \quad (\text{A5})$$

where  $s = q^2/(m_b^{1S})^2$ ,  $\hat{m}_c = m_c^{1S}/m_b^{1S}$ , and

$$t_i = \left( \frac{4}{3}, 1, 6, 0, 60, 0 \right), \quad u_i = \left( 0, 0, -\frac{7}{2}, -\frac{2}{3}, -38, -\frac{32}{3} \right), \quad w_i = \left( 0, 0, -\frac{1}{2}, -\frac{2}{3}, -8, -\frac{32}{3} \right). \quad (\text{A6})$$

The second line in  $F_9(q^2)$  arises from reexpanding the leading order contribution in the  $1S$  scheme. The one-loop function  $h(\hat{m}_c, s)$  encoding the four-quark contributions is [6, 13]

$$\begin{aligned} h(\hat{m}_c, s) &= -\frac{8}{9} \ln(\hat{m}_c) - \frac{4}{27} + \frac{2s}{9\hat{m}_c^2} - \frac{4}{9} \left( 1 + \frac{s}{2\hat{m}_c^2} \right) \mathcal{F}\left(\frac{s}{4\hat{m}_c^2}\right), \\ h(0, s) &= -\frac{4}{9} \ln(s) + \frac{8}{27} + \frac{4}{9} i\pi, \end{aligned} \quad (\text{A7})$$

and we have defined the function

$$\mathcal{F}(x) = 1 - \frac{1}{x} + \frac{\sqrt{|1-1/x|}}{x} \begin{cases} \arctan \sqrt{\frac{x}{1-x}}, & 0 < x < 1, \\ \ln(\sqrt{x} + \sqrt{x-1}) - i\pi/2, & x > 1. \end{cases} \quad (\text{A8})$$

It satisfies  $\mathcal{F}(0) = 2/3$  and  $\mathcal{F}(1-\epsilon) = \text{sgn}(\epsilon)(\pi/2)\sqrt{\epsilon} + \mathcal{O}(\epsilon)$ .

The one-loop functions  $f_8^{(7,9)}(s)$  in Eq. (A5) containing the  $O_8$  contributions are

$$\begin{aligned} f_8^{(7)}(s) &= -\frac{2}{9} \left[ \frac{4s}{1-s} \ln(s) + (22 + 60s + 158s^2 + 329s^3 + \dots) - (2 + 9s + 24s^2 + 50s^3 + \dots) \frac{2\pi^2}{3} + 4i\pi \right], \\ f_8^{(9)}(s) &= \frac{4}{9} \left[ \frac{4}{1-s} \ln(s) + \frac{1}{15} (390 + 1480s + 3553s^2 + \dots) - (4 + 15s + 36s^2 + \dots) \frac{2\pi^2}{3} \right]. \end{aligned} \quad (\text{A9})$$

Their exact analytic expressions in terms of integrals can be found in Refs. [15, 16]. Here we expanded the terms

not proportional to  $\ln(s)$  for small  $s$ . Since these are small compared with the  $\ln(s)$  term, the expressions above are

accurate to better than  $10^{-3}$  for  $s < 1$  and  $10^{-5}$  for  $s < 0.4$ .

The two-loop functions  $f_{1-6}^{(7,9)}$  in Eq. (A5) contain the virtual  $\mathcal{O}(\alpha_s)$  contributions from  $O_{1-6}$  and are known for  $i = 1$  and 2 only. In Ref. [14] they are given as expansions in  $s$  and  $\hat{m}_c$ . Since the expressions for general  $\hat{m}_c$  are quite lengthy, Ref. [14] also quotes them at five fixed values for  $\hat{m}_c$ , which we use together with a linear interpolation for intermediate values of  $\hat{m}_c$ .

Usually, the contributions from  $O_{1,2,8}$  that enter  $C_{7,9}^{\text{incl}}(q^2)$  are included via functions  $F_{1,2,8}^{(7,9)}$  [14]; e.g., for the  $O_1$  contribution to  $C_9^{\text{incl}}$

$$C_9^{\text{incl}} = C_9 - \frac{\alpha_s}{4\pi} C_1 F_1^{(9)} + \dots \quad (\text{A10})$$

The  $F_{1,2,8}^{(7,9)}$  consist of terms containing powers of  $\ln(\mu/m_b)$  and the functions  $f_{1,2,8}^{(7,9)}$ . For example, switching to the pole scheme, the terms proportional to  $\alpha_s/(4\pi)C_1$  are

$$\begin{aligned} F_1^{(9)} &= \ln \frac{\mu}{m_b} \left\{ \gamma_{1j}^{(0)} \kappa_{j9} + \gamma_{19}^{(1)} - \frac{1}{2} \gamma_{1j}^{(0)} \gamma_{j9}^{(0)} \ln \frac{\mu}{m_b} \right. \\ &\quad \left. + \gamma_{1j}^{(0)} [t_j h(\hat{m}_c, s) + u_j h(1, s) + w_j h(0, s)] \right\} + f_1^{(9)} \\ &= -\ln \frac{\mu}{m_b} \left[ \frac{256}{243} \ln \frac{\mu}{m_b} - \frac{2272}{729} - \frac{8}{3} h(\hat{m}_c, s) \right. \\ &\quad \left. + \frac{4}{27} h(1, s) + \frac{4}{27} h(0, s) \right] + f_1^{(9)}. \end{aligned} \quad (\text{A11})$$

In our scheme these  $\ln(\mu/m_b)$  dependent terms are split up between  $F_9(q^2)$  and  $C_i$ , and are included in the defi-

nitions (A2) and (A5). Expanding the term in brackets for small  $s$ , we recover the result given in Ref. [14]. The same is true for all  $F_{1,2,8}^{(7,9)}$ . Note that in this way we automatically include the  $\ln(\mu/m_b)$  dependent terms of the analogous functions  $F_{3-6}^{(7,9)}$ , which to our knowledge have not been calculated explicitly so far.

The functions  $G_{7,9}(q^2)$  contain  $\mathcal{O}(1/m_c^2)$  corrections in Eq. (11), calculated for  $d\Gamma/dq^2$  and  $dA_{\text{FB}}/dq^2$  in Ref. [12]. We found that their contribution can be included similarly to other four-quark operator contributions in  $C_{7,9}^{\text{incl}}(q^2)$  [see Eq. (11)] via the functions

$$\begin{aligned} G_9(q^2) &= \frac{10}{1-2s} G_7(q^2) \\ &= -\frac{5}{6} \left( C_2 - \frac{C_1}{6} \right) \frac{\lambda_2}{m_c^2} \frac{\mathcal{F}[q^2/(4m_c^2)]}{1 - q^2/(4m_c^2)}. \end{aligned} \quad (\text{A12})$$

(In the operator basis used in Ref. [12] the  $C_2 - C_1/6$  term in Eq. (A12) should be replaced by their  $C_2$ , and we set this coefficient to unity in our numerical analysis.) These corrections diverge as  $(4m_c^2 - q^2)^{-1/2}$  as  $q^2$  approaches the  $4m_c^2$  threshold. Following Ref. [12], we imagine that this calculation makes sense for  $q^2 \lesssim 3m_c^2 \approx 6 \text{ GeV}^2$ . Even for  $q^2 \ll 4m_c^2$ , there is an infinite series of corrections suppressed only by increasing powers of  $\Lambda m_b/m_c^2$  [42].

The  $\omega_i^j(s)$  containing the  $\mathcal{O}(\alpha_s)$  corrections in Eq. (13) can be extracted from Ref. [22]. Defining

$$L(s) = 4 \text{Li}_2(s) + 2 \ln(s) \ln(1-s) + \frac{2\pi^2}{3}, \quad (\text{A13})$$

we find

$$\begin{aligned} \omega_T^{99}(s) &= \frac{1}{2\sqrt{s}} \omega^{99}(s) + L(s) + \frac{1+2s}{s} \ln(1-s) + \frac{5+s(7-2s)}{(1-s)^2} \ln(s) + \frac{19+s}{2(1-s)} - \frac{1+3s}{1-s} \frac{\delta^{1S}(\mu)}{2}, \\ \omega_A^{90}(s) &= 2 \frac{1+s(3-s)}{(1-s)^2} \text{Li}_2(s) + \frac{1-s(9-2s)}{s(1-s)} \ln(1-s) - \frac{4s(5-2s)}{(1-s)^2} \text{Li}_2(\sqrt{s}) + \frac{2(5-2s)}{1-s} \ln(1-\sqrt{s}) \\ &\quad + \frac{2+s}{(1-s)^2} \frac{\pi^2}{3} - \frac{3-4\sqrt{s}}{(1+\sqrt{s})^2} - \frac{1+3s}{1-s} \frac{\delta^{1S}(\mu)}{2}, \\ \omega_L^{99}(s) &= -\sqrt{s} \omega^{99}(s) + L(s) + 3 \ln(1-s) - \frac{8s(1+2s)}{(1-s)^2} \ln(s) - \frac{5+s(47-4s)}{2(1-s)} - \frac{3+s}{1-s} \frac{\delta^{1S}(\mu)}{2}, \\ \omega^{99}(s) &= -4 \frac{5+s(12-s)}{(1-s)^2} \text{Li}_2(1-\sqrt{s}) + \frac{9-(2-\sqrt{s})^2}{(1-\sqrt{s})^2} \text{Li}_2(1-s) + \frac{9-(2+\sqrt{s})^2}{(1+\sqrt{s})^2} \frac{\pi^2}{2}, \end{aligned} \quad (\text{A14})$$

$$\begin{aligned} \omega_T^{77}(s) &= \frac{\sqrt{s}}{2} \omega^{77}(s) + L(s) + 3 \ln(1-s) - \frac{s(1+5s)}{(1-s)^2} \ln(s) - \frac{16+5s(5-s)}{6(1-s)} - \frac{3+s}{1-s} \frac{\delta^{1S}(\mu)}{2}, \\ \omega_L^{77}(s) &= -\frac{1}{\sqrt{s}} \omega^{77}(s) + L(s) + \frac{2+s}{s} \ln(1-s) + 2 \frac{3+s(3-s)}{(1-s)^2} \ln(s) + \frac{21-s}{2(1-s)} - \frac{1+3s}{1-s} \frac{\delta^{1S}(\mu)}{2}, \\ \omega^{77}(s) &= 4 \frac{12-(3-s)^2}{(1-s)^2} \text{Li}_2(1-\sqrt{s}) - \frac{4-(1-\sqrt{s})^2}{(1-\sqrt{s})^2} \text{Li}_2(1-s) - \frac{4-(1+\sqrt{s})^2}{(1+\sqrt{s})^2} \frac{\pi^2}{2}, \end{aligned} \quad (\text{A15})$$

$$\begin{aligned}
\omega_T^{79}(s) &= \frac{1}{2} \omega^{79}(s) + L(s) + \frac{1+5s}{2s} \ln(1-s) - \frac{s(1+3s)}{2(1-s)^2} \ln(s) - \frac{9-5s}{2(1-s)} - \frac{1+s}{1-s} \delta^{1S}(\mu), \\
\omega_A^{70}(s) &= \frac{3+s(9-2s)}{(1-s)^2} \text{Li}_2(s) + \frac{1-s(22-s)}{2s(1-s)} \ln(1-s) - 2 \frac{1+s(13-4s)}{(1-s)^2} \text{Li}_2(\sqrt{s}) + \frac{13-3s}{1-s} \ln(1-\sqrt{s}) \\
&\quad + \frac{5(1+s)}{2(1-s)^2} \frac{\pi^2}{3} - \frac{s+(3-2\sqrt{s})^2}{2(1+\sqrt{s})^2} - \frac{1+s}{1-s} \delta^{1S}(\mu), \\
\omega_L^{79}(s) &= -\omega^{79}(s) + L(s) + \frac{1+2s}{s} \ln(1-s) + \frac{s(7-s)}{(1-s)^2} \ln(s) + \frac{1+11s}{2(1-s)} - \frac{1+s}{1-s} \delta^{1S}(\mu), \\
\omega^{79}(s) &= 4 \frac{\sqrt{s}(3+s)}{(1-s)^2} \text{Li}_2(1-\sqrt{s}) - \frac{1+\sqrt{s}}{(1-\sqrt{s})^2} \text{Li}_2(1-s) + \frac{1-\sqrt{s}}{(1+\sqrt{s})^2} \frac{\pi^2}{2}.
\end{aligned} \tag{A16}$$

The functions  $\omega^i(s)$  entering  $\omega_{T,L}^i(s)$  contain all the dependence on  $\sqrt{s}$ , which cancels in the  $q^2$  spectrum. All  $\ln(\mu/m_b)$  terms that usually appear in the functions  $\omega_i^{77,79}(s)$  have been moved into  $\mathcal{C}_7$  (along with the appropriate constant term contained in  $\overline{m}_b/m_b^{1S}$ ).

The  $\chi_i^j(s)$  containing the  $\mathcal{O}(1/m_b^2)$  corrections in Eq. (13) can be extracted from Ref. [24]:

$$\begin{aligned}
\chi_T^{99}(s) &= -\frac{\lambda_1 + 3\lambda_2}{6} \frac{5+3s}{1-s} - 2\lambda_2 \frac{s(4-3s)}{(1-s)^2}, \\
\chi_A^{90}(s) &= \frac{\lambda_1 + 3\lambda_2}{6} \frac{3+s(2+3s)}{(1-s)^2} - 2\lambda_2 \frac{3+s(4-3s)}{(1-s)^2}, \\
\chi_L^{99}(s) &= \frac{\lambda_1 + 3\lambda_2}{6} \frac{3+13s}{1-s} - 2\lambda_2 \frac{s^2}{(1-s)^2}, \\
\chi_T^{77}(s) &= \frac{\lambda_1 + 3\lambda_2}{6} \frac{3+5s}{1-s} - 2\lambda_2 \frac{3-2s^2}{(1-s)^2}, \\
\chi_L^{77}(s) &= -\frac{\lambda_1 + 3\lambda_2}{6} \frac{13+3s}{1-s} - 2\lambda_2 \frac{s(4-3s)}{(1-s)^2}, \\
\chi_T^{79}(s) &= \frac{\lambda_1 + 3\lambda_2}{2} - \lambda_2 \frac{5-3s^2}{(1-s)^2}, \\
\chi_A^{70}(s) &= \frac{\lambda_1 + 3\lambda_2}{6} \frac{3+s(2+3s)}{(1-s)^2} - \lambda_2 \frac{5+3s(2-s)}{(1-s)^2}, \\
\chi_L^{79}(s) &= \frac{\lambda_1 + 3\lambda_2}{2} - 2\lambda_2 \frac{1}{(1-s)^2}.
\end{aligned} \tag{A17}$$

## APPENDIX B: NUMERICAL INPUTS

In this Appendix we collect all of our numerical inputs. All values are taken from Ref. [38] except where stated otherwise. To evaluate the Wilson coefficients we use

$$\begin{aligned}
m_W &= 80.403 \text{ GeV}, \\
\sin^2 \theta_W &= 0.23122, \\
m_t^{\text{pole}} &= (171.4 \pm 2.1) \text{ GeV}, \\
\alpha_s(m_Z) &= 0.1176, \\
\mu_0^c &= 80 \text{ GeV}, \\
\mu_0^t &= 120 \text{ GeV}.
\end{aligned} \tag{B1}$$

	$\mu = 2.35 \text{ GeV}$	$\mu = 4.7 \text{ GeV}$	$\mu = 9.4 \text{ GeV}$
$\alpha_s(\mu)$	0.2659	0.2140	0.1793
$C_1(\mu)$	-0.4642	-0.2880	-0.1506
$C_2(\mu)$	1.019	1.007	1.001
$C_3(\mu)$	-0.0096	-0.0043	-0.0017
$C_4(\mu)$	-0.1247	-0.0795	-0.0508
$C_5(\mu)$	0.00069	0.00029	0.00009
$C_6(\mu)$	0.00205	0.00081	0.00026
$C_8(\mu)$	-0.2012	-0.1778	-0.1598
$\overline{m}_b(\mu)$	4.703	4.120	3.707
$C_7(\mu)$	-0.3637	-0.3293	-0.2982
$\mathcal{C}_7$	-0.2435	-0.2611	-0.2687
$C_9(\mu)$	4.504	4.209	3.790
$\mathcal{C}_9$	4.258	4.207	4.188
$\mathcal{C}_{10}$	-4.175	-4.175	-4.175

TABLE I: Values of the Wilson coefficients to  $\mathcal{O}(\alpha_s)$  at different low scales  $\mu$ .

Here,  $\mu_0^{c,t}$  are the matching scales in the charm and top sector, respectively, and we use the same values as in Ref. [19]. For the top quark mass we use the newest CDF and D0 average [43]. The resulting values for the Wilson coefficients at  $\mathcal{O}(\alpha_s)$  run down to the low scale and the corresponding values for the  $\mathcal{C}_i$  according to Eq. (A2) are listed in Table I. Note that the residual scale uncertainties of  $\mathcal{C}_7$  and especially  $\mathcal{C}_9$  are much smaller than those of  $C_{7,9}(\mu)$ . We use a Mathematica code by Bobeth with the initial conditions and renormalization group running as given in Refs. [19, 20]. For  $\mathcal{C}_9(\mu)$  this requires the three-loop mixings calculated in Refs. [44].

In the decay rates we use

$$\begin{aligned}
\alpha_{\text{em}}(m_b) &= 1/133, \\
|V_{tb}V_{ts}^*| &= 41.09 \times 10^{-3}, \\
m_B &= 5.279 \text{ GeV}, \\
\tau_B &= 1.584 \text{ ps}, \\
m_{K^*} &= 0.892 \text{ GeV}, \\
m_b \equiv m_b^{1S} &= (4.70 \pm 0.04) \text{ GeV},
\end{aligned}$$

$$\begin{aligned}
m_c &\equiv m_c^{1S} = (1.41 \pm 0.05) \text{ GeV}, \\
\lambda_1 &= -0.27 \text{ GeV}^2, \\
\lambda_2 &= 0.12 \text{ GeV}^2.
\end{aligned} \tag{B2}$$

We use the value of the electromagnetic coupling at the scale  $\mu \sim m_b$ , because for the total rate in this case the higher order electroweak corrections (which we neglect in our analysis) turn out to be numerically small, below

the two percent level [20, 28]. The value of  $|V_{tb}V_{ts}^*|$  is taken from Ref. [1]. For  $m_b^{1S}$  we take the naive average of Refs. [27, 45], which coincides with the PDG average [38], and use the average of the errors quoted in Refs. [27, 45]. For  $m_c^{1S}$  we use the result of Ref. [46] as quoted in the 1S scheme in Ref. [1]. Finally, for  $\lambda_1$  we take the value from Ref. [27], and  $\lambda_2 = (m_{B^*}^2 - m_B^2)/4 \approx 0.12 \text{ GeV}^2$ .

- 
- [1] For a recent review, see: A. Höcker and Z. Ligeti, *Ann. Rev. Nucl. Part. Sci.* **56**, 501 (2006) [hep-ph/0605217].
- [2] B. Aubert *et al.* [BABAR Collaboration], *Phys. Rev. Lett.* **93**, 081802 (2004) [hep-ex/0404006].
- [3] M. Iwasaki *et al.* [Belle Collaboration], *Phys. Rev. D* **72**, 092005 (2005) [hep-ex/0503044].
- [4] K. Abe *et al.* [Belle Collaboration], hep-ex/0410006; A. Ishikawa *et al.*, *Phys. Rev. Lett.* **96**, 251801 (2006) [hep-ex/0603018].
- [5] B. Aubert *et al.* [BABAR Collaboration], *Phys. Rev. D* **73**, 092001 (2006) [hep-ex/0604007].
- [6] B. Grinstein, M. J. Savage and M. B. Wise, *Nucl. Phys. B* **319**, 271 (1989).
- [7] A. Ali, T. Mannel and T. Morozumi, *Phys. Lett. B* **273**, 505 (1991).
- [8] P. L. Cho, M. Misiak and D. Wyler, *Phys. Rev. D* **54**, 3329 (1996) [hep-ph/9601360].
- [9] A. H. Hoang, Z. Ligeti and A. V. Manohar, *Phys. Rev. Lett.* **82** (1999) 277 [hep-ph/9809423]; *Phys. Rev. D* **59**, 074017 (1999) [hep-ph/9811239].
- [10] J. L. Hewett, *Phys. Rev. D* **53**, 4964 (1996) [hep-ph/9506289]; F. Krüger and L. M. Sehgal, *Phys. Lett. B* **380**, 199 (1996) [hep-ph/9603237]; W. Bensalem, D. London, N. Sinha and R. Sinha, *Phys. Rev. D* **67**, 034007 (2003) [hep-ph/0209228].
- [11] F. Krüger and J. Matias, *Phys. Rev. D* **71**, 094009 (2005) [hep-ph/0502060]; D. Melikhov, N. Nikitin and S. Simula, *Phys. Lett. B* **442**, 381 (1998) [hep-ph/9807464]; F. Krüger, L. M. Sehgal, N. Sinha and R. Sinha, *Phys. Rev. D* **61**, 114028 (2000) [Erratum-ibid. *D* **63**, 019901 (2001)] [hep-ph/9907386].
- [12] G. Buchalla, G. Isidori and S. J. Rey, *Nucl. Phys. B* **511**, 594 (1998) [hep-ph/9705253].
- [13] M. Misiak, *Nucl. Phys. B* **393** (1993) 23 [Erratum-ibid. *B* **439** (1995) 461]; A. J. Buras and M. Münz, *Phys. Rev. D* **52**, 186 (1995) [hep-ph/9501281].
- [14] H. H. Asatryan, H. M. Asatrian, C. Greub and M. Walker, *Phys. Lett. B* **507**, 162 (2001) [hep-ph/0103087]; *Phys. Rev. D* **65** (2002) 074004 [hep-ph/0109140].
- [15] M. Beneke, T. Feldmann and D. Seidel, *Nucl. Phys. B* **612**, 25 (2001) [hep-ph/0106067].
- [16] A. Ghinculov, T. Hurth, G. Isidori and Y. P. Yao, *Nucl. Phys. B* **685** (2004) 351 [hep-ph/0312128].
- [17] K. Adel and Y. P. Yao, *Phys. Rev. D* **49**, 4945 (1994) [hep-ph/9308349]; C. Greub and T. Hurth, *Phys. Rev. D* **56**, 2934 (1997) [hep-ph/9703349].
- [18] K. G. Chetyrkin, M. Misiak and M. Münz, *Phys. Lett. B* **400**, 206 (1997) [Erratum-ibid. *B* **425**, 414 (1998)] [hep-ph/9612313].
- [19] C. Bobeth, M. Misiak and J. Urban, *Nucl. Phys. B* **574** (2000) 291 [hep-ph/9910220].
- [20] C. Bobeth, P. Gambino, M. Gorbahn and U. Haisch, *JHEP* **0404** (2004) 071 [hep-ph/0312090].
- [21] A. Ghinculov, T. Hurth, G. Isidori and Y. P. Yao, *Nucl. Phys. B* **648** (2003) 254 [hep-ph/0208088].
- [22] H. M. Asatrian, K. Bieri, C. Greub and A. Hovhannisyan, *Phys. Rev. D* **66** (2002) 094013 [hep-ph/0209006].
- [23] A. F. Falk, M. E. Luke and M. J. Savage, *Phys. Rev. D* **49**, 3367 (1994) [hep-ph/9308288].
- [24] A. Ali, G. Hiller, L. T. Handoko and T. Morozumi, *Phys. Rev. D* **55**, 4105 (1997) [hep-ph/9609449].
- [25] H. H. Asatryan, H. M. Asatrian, C. Greub and M. Walker, *Phys. Rev. D* **66**, 034009 (2002) [hep-ph/0204341].
- [26] H. H. Asatryan, H. M. Asatrian, A. Hovhannisyan and V. Poghosyan, *Mod. Phys. Lett. A* **19**, 603 (2004) [hep-ph/0311187].
- [27] C. W. Bauer, Z. Ligeti, M. Luke, A. V. Manohar and M. Trott, *Phys. Rev. D* **70**, 094017 (2004) [hep-ph/0408002].
- [28] T. Huber, E. Lunghi, M. Misiak and D. Wyler, *Nucl. Phys. B* **740**, 105 (2006) [hep-ph/0512066].
- [29] C. W. Bauer, S. Fleming and M. E. Luke, *Phys. Rev. D* **63**, 014006 (2001) [hep-ph/0005275]; C. W. Bauer, S. Fleming, D. Pirjol and I. W. Stewart, *Phys. Rev. D* **63**, 114020 (2001) [hep-ph/0011336]; C. W. Bauer and I. W. Stewart, *Phys. Lett. B* **516**, 134 (2001) [hep-ph/0107001]; C. W. Bauer, D. Pirjol and I. W. Stewart, *Phys. Rev. D* **65**, 054022 (2002) [hep-ph/0109045].
- [30] C. W. Bauer, D. Pirjol, I. Z. Rothstein and I. W. Stewart, *Phys. Rev. D* **70**, 054015 (2004) [hep-ph/0401188].
- [31] J. Charles, A. Le Yaouanc, L. Oliver, O. Pene and J. C. Raynal, *Phys. Rev. D* **60**, 014001 (1999) [hep-ph/9812358].
- [32] A. Ali, P. Ball, L. T. Handoko and G. Hiller, *Phys. Rev. D* **61**, 074024 (2000) [hep-ph/9910221].
- [33] D. Pirjol and I. W. Stewart, hep-ph/0309053.
- [34] A. Ali, G. Kramer and G. h. Zhu, *Eur. Phys. J. C* **47**, 625 (2006) [hep-ph/0601034].
- [35] B. O. Lange and M. Neubert, *Nucl. Phys. B* **690**, 249 (2004) [Erratum-ibid. *B* **723**, 201 (2005)] [hep-ph/0311345].
- [36] A. V. Manohar and I. W. Stewart, hep-ph/0605001.
- [37] O. Schneider, Talk at the “Flavour in the era of the LHC” workshop, Nov. 2005, CERN, <http://indico.cern.ch/conferenceDisplay.py?confId=a052129>.
- [38] W. M. Yao *et al.* [Particle Data Group], *J. Phys. G* **33**, 1 (2006).
- [39] S. W. Bosch and G. Buchalla, *Nucl. Phys. B* **621**, 459

- (2002) [hep-ph/0106081].
- [40] K. S. M. Lee, Z. Ligeti, I. W. Stewart and F. J. Tackmann, Phys. Rev. D **74**, 011501 (2006) [hep-ph/0512191]; K. S. M. Lee and I. W. Stewart, Phys. Rev. D **74**, 014005 (2006) [hep-ph/0511334].
  - [41] G. Buchalla, A. J. Buras and M. E. Lautenbacher, Rev. Mod. Phys. **68**, 1125 (1996) [hep-ph/9512380].
  - [42] Z. Ligeti, L. Randall and M. B. Wise, Phys. Lett. B **402**, 178 (1997) [hep-ph/9702322].
  - [43] E. Brubaker *et al.* [Tevatron Electroweak Working Group], hep-ex/0608032.
  - [44] P. Gambino, M. Gorbahn and U. Haisch, Nucl. Phys. B **673**, 238 (2003) [hep-ph/0306079]; M. Gorbahn and U. Haisch, Nucl. Phys. B **713**, 291 (2005) [hep-ph/0411071].
  - [45] K. Abe *et al.* [Belle Collaboration], hep-ex/0611047.
  - [46] A. H. Hoang and A. V. Manohar, Phys. Lett. B **633**, 526 (2006) [hep-ph/0509195].